Geophysical Research Letters

RESEARCH LETTER
10.1029/2024GL111638

Midlatitude Plasma Blob-like Structures Along With Super Equatorial Plasma Bubbles During the May 2024 Great Geomagnetic Storm

Wenjie Sun[1,2], Guozhu Li[1,2,3], Biqiang Zhao[1,2,3], Shun-Rong Zhang[4], Yuichi Otsuka[5], Lianhuan Hu[1,2], Guofeng Dai[1,2], Xiukuan Zhao[2,6], Haiyong Xie[1,2,3], Yi Li[1,2], Jianfei Liu[1,2], Yu Li[7], Baiqi Ning[1,2], Libo Liu[2,3,6], Atsuki Shinbori[5], Michi Nishioka[8], and Septi Perwitasari[8]

[1]Beijing National Observatory of Space Environment, Institute of Geology and Geophysics, Chinese Academy of Sciences, Beijing, China, [2]Key Laboratory of Earth and Planetary Physics, Institute of Geology and Geophysics, Chinese Academy of Sciences, Beijing, China, [3]College of Earth and Planetary Sciences, University of Chinese Academy of Sciences, Beijing, China, [4]Haystack Observatory, Massachusetts Institute of Technology, Westford, MA, USA, [5]Institute for Space-Earth Environmental Research, Nagoya University, Nagoya, Japan, [6]Heilongjiang Mohe National Observatory of Geophysics, Institute of Geology and Geophysics, Chinese Academy of Sciences, Beijing, China, [7]China Earthquake Networks Center, China Earthquake Administration, Beijing, China, [8]National Institute of Information and Communications Technology, Tokyo, Japan

Abstract Plasma blob is generally a low-latitude phenomenon occurring at the poleward edge of equatorial plasma bubble (EPB) during post-sunset periods. Here we report a case of midlatitude ionospheric plasma blob-like structures occurring along with super EPBs over East Asia around sunrise during the May 2024 great geomagnetic storm. Interestingly, the blob-like structures appeared at both the poleward and westward edges of EPBs, reached up to 40°N magnetic latitudes, and migrated westward several thousand kilometers together with the bubble. The total electron content (TEC) inside the blob-like structures was enhanced by ∼50 TEC units relative to the ambient ionosphere. The blob-like structure at the EPB poleward edge could be partly linked with field-aligned plasma accumulation due to poleward development of bubble. For the blob-like structure at the EPB west side, one possible mechanism is that it was formed and enhanced accompanying the bubble evolution and westward drift.

Plain Language Summary Accompanying the generation of equatorial plasma bubble (EPB), an extra structure with plasma density enhancement may occur. The density-enhanced structure is known as plasma blob. Generally, plasma blobs mainly appear at the poleward edge of EPB, being low-latitude phenomena occurring at 10–20° magnetic latitudes. Whereas previous simulations showed that plasma blobs could appear at the east/west side of EPBs, there were few observational evidences and the driving mechanism is unclear. In this study, midlatitude plasma blob-like structures occurring up to 40°N magnetic latitude was observed along with super EPBs during magnetic storm. Different from most blobs appearing at the EPB poleward edge, the blob-like structures in the present study appeared at both the EPB poleward and westward edges. By using ground-based observations from GNSS receiver networks and in-situ measurements onboard spacecraft, the morphology and evolution of the super plasma blob-like structures are visualized. Potential mechanisms responsible for their generation are investigated. The results highlight the coexistence of large-scale plasma depletion and blob structures and their complex evolution with longitude and latitude, and have implications for better understanding the sudden changes of plasma density in time and altitude observed by radar.

Key Points:

- Super plasma blob-like structures occurred up to 40°N MLat along with equatorial plasma bubbles near sunrise during storm time
- The blob-like structures mainly occurred at the bubble poleward and westward edges and migrated westward along with the bubble
- The poleward development and evolution of the bubble could contribute to the formation of super blob-like structures

Supporting Information:

Supporting Information may be found in the online version of this article.

Correspondence to:

G. Li,
gzlee@mail.iggcas.ac.cn

Citation:

Sun, W., Li, G., Zhao, B., Zhang, S.-R., Otsuka, Y., Hu, L., et al. (2024). Midlatitude plasma blob-like structures along with super equatorial plasma bubbles during the May 2024 great geomagnetic storm. *Geophysical Research Letters*, *51*, e2024GL111638. https://doi.org/10.1029/2024GL111638

Received 27 JUL 2024
Accepted 18 OCT 2024

1. Introduction

The occurrences of ionospheric plasma bubbles (EPBs) usually create a region with plasma density depletion. Along with the EPB depletion structure, a plasma density enhancement structure may form, usually termed as plasma blob (Le et al., 2003; Oya et al., 1986; Park et al., 2003). Plasma blobs could appear simultaneously at magnetically conjugate locations in opposite hemispheres, with field-aligned structures spanning several hundred kilometers (e.g., Park et al., 2008; Pimenta et al., 2004; Yokoyama et al., 2007). Their formation was suggested to be related to the upwelling and poleward developing processes of EPB structures, which first push the plasma

upward and then poleward along the magnetic field lines, and finally lead to plasma accumulation at the EPB poleward sides (e.g., Huang et al., 2014; Wang et al., 2015).

The plasma blobs accompanying EPBs are expected to appear at the poleward edge of EPB structures, generally being a low-latitude phenomenon at the latitudes 10–20° away from the magnetic equator (e.g., Haaser et al., 2012; Kim & Hegai, 2016; Klenzing et al., 2011; Park et al., 2022). It is known that under certain conditions, for example, during magnetic storms, EPBs could extend to middle latitudes, usually termed as super EPBs (e.g., Huang et al., 2007; Li et al., 2009; Ma & Maruyama, 2006; Sun et al., 2024). However, it is still not clear whether plasma blob could form at middle latitudes associated with super EPBs or not, and how the spatial morphology of such plasma blob evolves. Whereas plasma blobs were occasionally observed at middle latitudes, they were suggested to be associated with traveling ionospheric disturbances (TIDs) rather than EPBs (e.g., Kil et al., 2019). On the other hand, besides the EPB poleward edge, previous numerical simulations showed that plasma density enhancement could appear at the east or west side of EPBs (e.g., Huba & Liu, 2020; Yokoyama et al., 2015). However, there are few observational evidences, and the underlying mechanism is still unclear.

In this study, we report a case of unusual plasma blob-like structures extending to 40°N magnetic latitudes around sunrise over East Asia, being along with super EPBs observed during the May 2024 great geomagnetic storm. Different from most blobs that usually form at the EPB poleward edge, the blob-like structures in the present case appeared at both the poleward and westward edges of super EPB. Based on dense observations from Global Navigation Satellite System (GNSS) receiver networks, in combination with in-situ observations onboard multiple spacecraft, the morphology and evolution of the super blob-like structures are visualized. The potential mechanisms responsible for their generation are discussed.

2. Data and Methods

The ground-based GNSS receiver networks employed in the present study include the Ionospheric Observational Network for Irregularity and Scintillation in East/Southeast Asia (IONISE) (Li et al., 2019; Sun et al., 2020), the Crustal Movement Observation Network of China (CMONOC; Aa et al., 2015), the International GNSS Service (IGS) Working Group on ionosphere (Beutler et al., 1999), the Geoscience Australia network (https://www.ga.gov.au) and the Chinese Meridian project (C. Wang, 2010). By tracking the signals of GNSS satellites, the vertical total electron content (TEC) with 30 s sampling rate was calculated, in a similar way to our previous studies (e.g., Sun et al., 2023). The rate of TEC change (ROT) is used to indicate the increase and decrease of TEC. The rate of TEC index (ROTI; Pi et al., 1997) is used to characterize the irregularities associated with EPBs. TEC, ROT and ROTI are projected at 300 km altitude and binned into $1° \times 1°$ grids every 5 min. In addition, the online grid TEC and ROTI products by Nagoya University (https://stdb2.isee.nagoya-u.ac.jp/GPS/GPS-TEC/) are also assimilated in the present analysis.

The in-situ plasma density profiles obtained from the Swarm satellite A (Friis-Christensen et al., 2008; Xiong et al., 2019) and Defense Meteorological Satellite Program (DMSP) spacecraft F18 (Heelis & Coley, 2007; Huang et al., 2010) are used to investigate the occurrences of blob-like structures and EPBs at the altitudes ~470 km and at ~840 km, respectively. The plasma drift measured by DMSP spacecraft in the left direction relative to its orbit is also employed in the present analysis. Since the angle between the orbit and the magnetic meridian is relatively small in the Asian-Australian sector (e.g., Zhao et al., 2019), the left drift component is used to approximately indicate the plasma drift in the zonal direction.

3. Results

Figure 1 presents sequences of TEC and ROTI maps over the Asian-Australian sector. Four main features could be seen. (a) A large TEC enhancement structure appeared around 15–40°N magnetic latitudes near sunrise, with TEC increased by up to 50 TECu relative to the background ionosphere. The structure sometimes formed an outline with boundaries at the poleward (marked as "X") and westward (marked as "Y") directions, for example, around 20:00 universal time (UT, Beijing local time LT = UT + 8 hr). In the southern hemisphere at 15–40°S magnetic latitudes, TEC enhancement also occurred. (b) The ROTI inside the region surrounded by TEC enhancement is predominantly large. The large ROTI extended to nearly ±40° magnetic latitudes, and were associated with amplitude scintillation and VHF radar backscatter echoes (as shown in Figures 1S and 2S in the Supporting Information S1), indicating the occurrence of super EPBs. Three EPB structures marked as "A", "B" and "C" respectively could be roughly identified. EPB "A" has been well developed as a super bubble when it

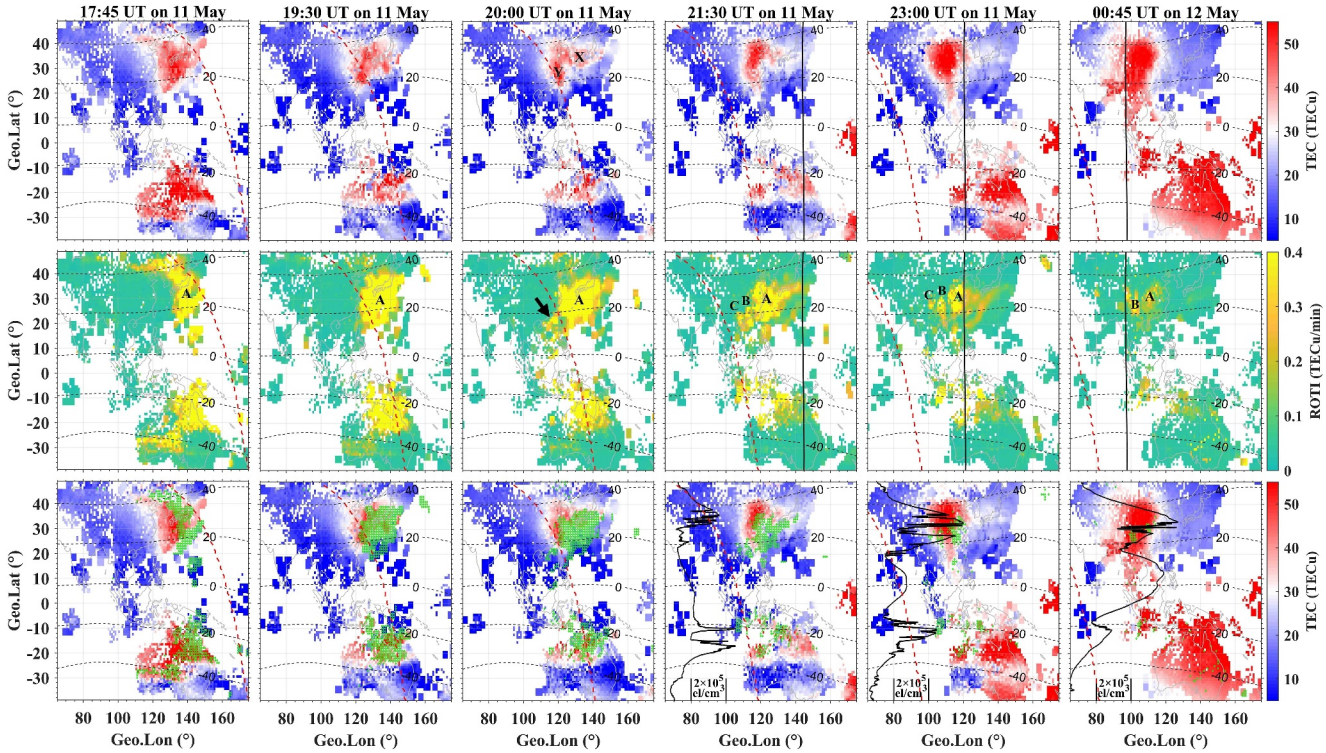

Figure 1. Sequences of (top) TEC and (middle) ROTI maps showing the evolution of blob-like structures and EPB irregularities. In the bottom panels, the locations with ROTI higher than 0.25 TECu/min are marked as green dots on the TEC maps. The superimposed black curves in the bottom right three panels denote the latitude profiles of in-situ plasma density observed by the Swarm satellite A at ∼470 km altitude around the time intervals of the TEC maps. The corresponding paths of Swarm A are marked in the top and middle panels. In each panel, the red dashed curve denotes the sunrise terminator at the altitude 300 km. The black dashed contours denote the magnetic dip latitudes.

entered the field-of-view of the ROTI maps (e.g., 17:45 UT), whereas EPBs "B" and "C" were still growing at 110–120°E (e.g., indicated by the black arrow at 20:00 UT) and finally reached ∼30° magnetic latitude (e.g., 23:00 UT). (c) From the bottom panels, the TEC enhancement region was mainly located at the poleward and westward sides of EPB "A" and migrated westward together with the EPB. Some EPB irregularities were embedded in the TEC enhancements, but the boundaries of the TEC enhancement region were almost beyond the edges of the EPB. During the process, the TEC enhancement structures continued developing, whereas the EPB gradually decayed. (d) When the Swarm satellite A passed the TEC enhancement region embedded by EPB irregularities (e.g., around 21:30, 23:00 and 00:45 UT), the in-situ plasma density (at the altitude ∼470 km) at the corresponding latitudes sometimes enhanced with depletion-like fluctuations. The TEC and in-situ plasma density enhancements observed in Figure 1 were similar to the plasma blobs associated with EPBs presented in previous studies (e.g., Park et al., 2022). Different from the blobs in previous studies that mainly appeared at low latitudes, the present TEC enhancement structures extended to middle latitudes more than 40°N.

Figure 2 shows the ROTI and TEC keograms along 20°N ± 10°, TEC along 37°N, and the SYM-H on 10–12 May 2024. A great geomagnetic storm occurred during the period, with a minimum SYM-H of −518 nT. Details of the storm evolution could be seen in Spogli et al. (2024) and will not be repeated here. On the previous day before the case (10 May), EPBs also occurred, which were normal post-sunset EPBs constrained at low latitudes and drifting eastward. For the EPBs on 11 May, they were observed around sunrise over the Asian-Australian sector (during the recovery stage of the May 2024 great geomagnetic storm) and mainly drifted westward. EPBs occurring around sunrise during geomagnetic storms have been previously investigated, which could be driven by storm-time electric fields and/or equatorward neutral wind (e.g., Otsuka et al., 2021; Sun et al., 2023) and will not be further discussed here. For the EPB structure "A", the present ROTI data could not trace its onset. It may be initiated over the longitudes more eastern than 150°E at the time earlier than 14:00 UT and drifted westward, as indicated by the black arrow in Figure 2a. The TEC enhancement structures were mainly associated with the EPB "A" but appeared at more western longitudes than the EPB. They migrated westward along with the EPB "A"

10.1029/2024GL111638

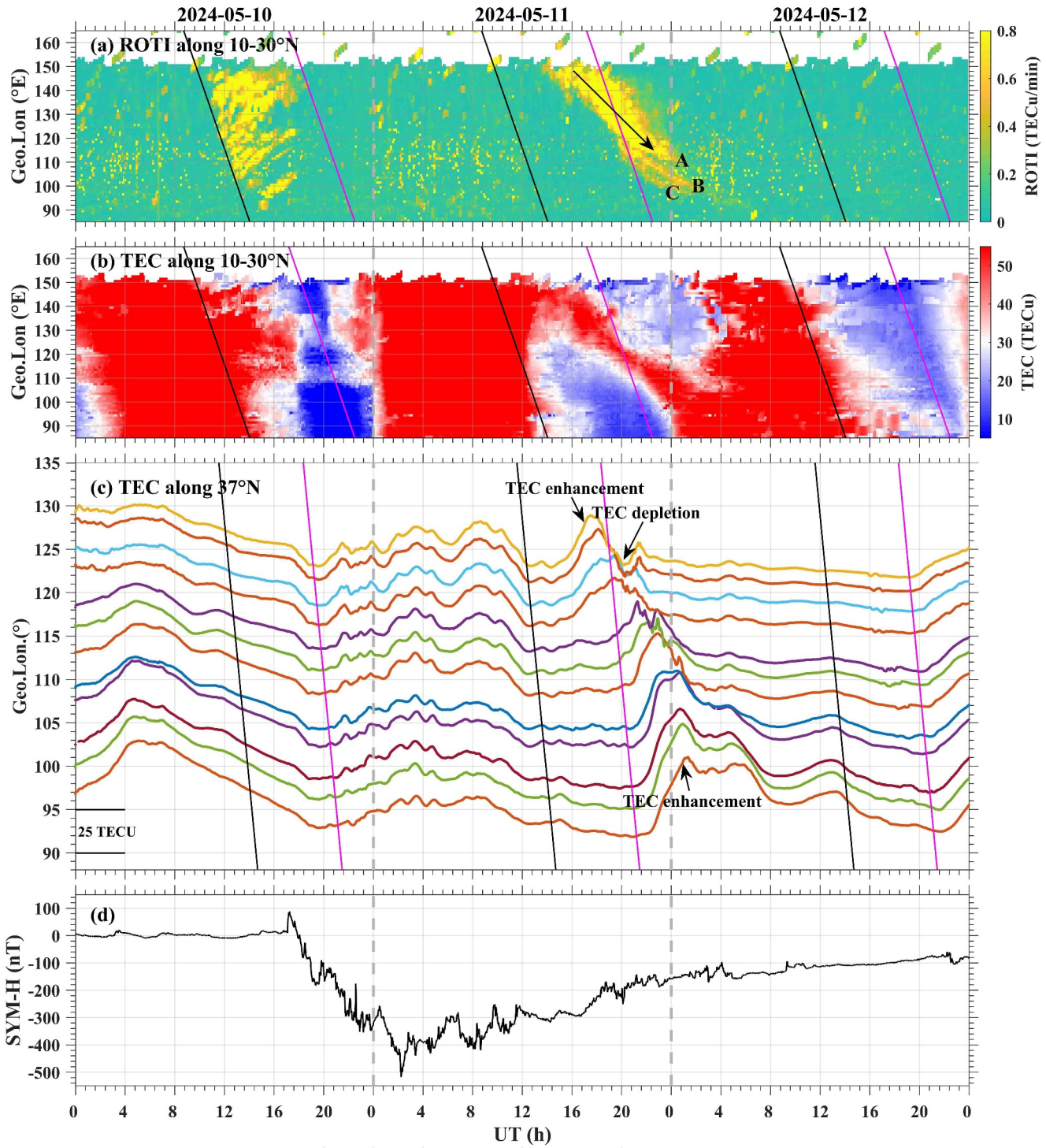

Figure 2. The keograms of (a) ROTI and (b) TEC along 10–30°N, (c) the TEC observed at the fixed IPPs of Beidou Geostationary satellites along 37°N, and (d) the SYM-H during 10–12 May 2024. In each grid (5 min × 1° in longitude) in (a) and (b), the TEC and ROTI are selected as the maximum values at 10–30°N. The black and magenta curves indicate the sunset and sunrise time, respectively.

across ∼5,000 km (from ∼140°E to ∼90°E) during ∼13:00–24:00 UT. The average migration velocity is estimated ∼126 m/s.

Notably, the TEC and ROTI maps in Figures 1 and 2 are projected at the same altitude 300 km, whereas the TEC enhancement structures and EPBs may actually occur at different altitudes. In this regard, we tested projecting TEC and ROTI at multiple different altitudes (figure not shown). The results indicate that when projecting at different altitudes, the TEC enhancement structures were still mainly at the EPB poleward and westward sides. Figure 2c presents the TEC continuously observed at the fixed ionospheric pierce points (IPPs) along 37°N via tracking Beidou Geostationary (BD-GEO) satellites. At each fixed IPP, TEC enhancement generally occurred earlier than TEC depletion caused by EPB. This was consistent with the fact that the TEC enhancement structures were located at the west side of the EPB, considering the major westward migration of the structures.

4. Discussion

The TEC enhancement structures in the present study were observed around sunrise over East Asia during the recovery stage of the May 2024 great geomagnetic storm. They were first observed at ∼150°E and migrated westward along with the super EPB, manifested as enhancements in TEC (up to ∼50 TECu) from low to middle latitudes (15–40° magnetic latitudes). Due to the data gaps at the more eastern longitudes over the Pacific oceans, their initial generation could not be well traced. One may argue that the TEC enhancement could be due to the sunrise effect. However, the occurrence of the TEC enhancement did not follow the sunrise at different longitudes, which initiated before sunrise at the eastern longitudes and migrated westward in a speed obviously smaller than the sunrise terminator (Figure 2b). Other possibilities responsible for TEC enhancement at middle latitudes include storm enhanced density (SED) structures (e.g., Foster, 1993), blobs associated with TIDs (e.g., Kil et al., 2019), and the storm-induced plasma stream (SIPS) structures (e.g., Maruyama et al., 2013). However, SED structures are usually observed in local afternoon and dusk sectors during early stages of geomagnetic storms (e.g., Aa et al., 2024), whereas the present case was observed around sunrise during the storm recovery stage. Plasma blobs associated with TIDs usually have well aligned wave fronts and propagate equatorward (e.g., Kil et al., 2019). Such features were not observed for the present case. SIPS were usually observed shortly after sunset, with an elongating structure connected to a TEC maximum root region at the dayside low latitudes (Maruyama et al., 2013). However, the TEC enhancement in the present case appeared as prominent structures isolated from the ambient ionosphere. Therefore, the TEC enhancement structures observed in the present study were unlikely due to SED, TIDs, or SIPS.

Generally, the present TEC enhancement structures are similar to the blobs associated with EPBs, mainly in the following aspects. Their occurrences and movement were along with the super EPB, with specific morphology surrounding the EPB structure (e.g., 20:00 UT in Figure 1). The TEC enhancement region that occurred at the poleward edge of the EPB structure is consistent with the blobs observed in previous studies (e.g., Park et al., 2022). However, the in-situ plasma density did not always exhibit blob-like signatures when the satellites seemed traveling through the TEC enhancement region. We have also sought for blob-like signatures in electron temperature profiles as shown in Figure S3 of the Supporting Information S1, but could not always find conspicuous blob signals, that is, decreased electron temperature associated with steep-gradient density enhancement as in previous studies (e.g., Choi et al., 2012, Figure 1; Park et al., 2003, Figure 1). There could be two possibilities for the discrepancy between TEC and in-situ plasma density. One is the temporal/longitudinal offset between the center of the blob-like structures and the satellite orbits. For example, the DMSP satellites would take ∼25 min to fly over the TEC map region, during which the blob-like structures may experience considerable evolution or drift. The other possibility is the altitude difference between the TEC data and in-situ measurements. The TEC data are projected at 300 km altitude whereas the orbits of the Swarm and DMSP satellites are at ∼470 and ∼840 km respectively.

Comparing with previous studies, the new points for the present blob-like structures mainly include two aspects. (a) The plasma blobs associated with EPBs in previous studies were mainly constrained at low latitudes 10–20° away from the magnetic equator (e.g., Kim & Hegai, 2016; Klenzing et al., 2011), whereas the present blob-like structures occurred up to 40°N magnetic latitudes. (b) The blob-like structures in the present case appeared at both the poleward and west sides of EPB structures, whereas in previous studies they mainly occurred at the EPB poleward edges (e.g., Huang et al., 2014; Park et al., 2022; Wang et al., 2019).

10.1029/2024GL111638

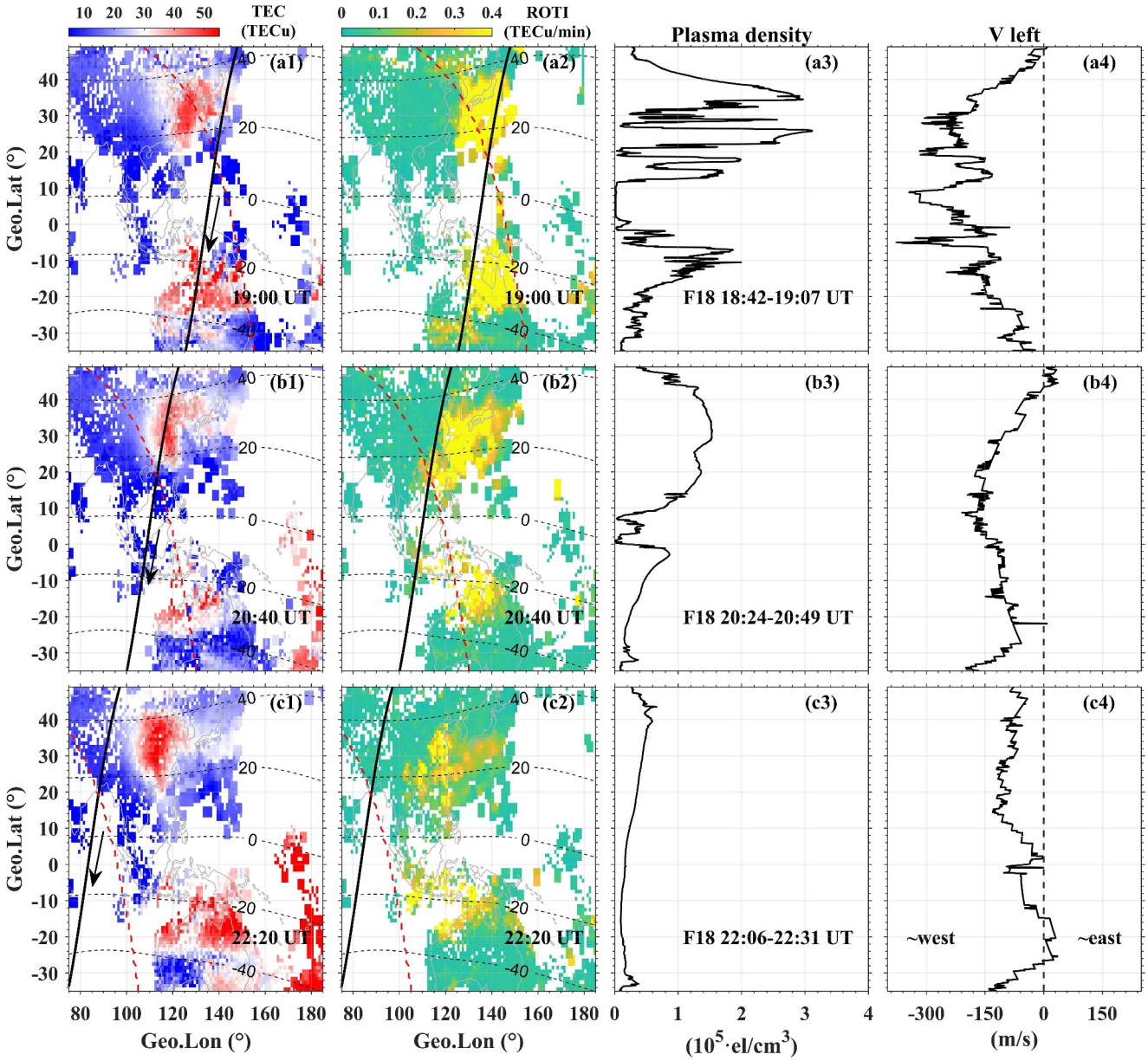

Figure 3. The panels from left to right are the TEC maps, ROTI maps, plasma density profiles, and ion drifts in the left direction relative to the satellite paths observed by the DMSP satellite F18 at ~840 km around three typical time intervals (top) 19:00 UT, (middle) 20:40 UT and (bottom) 22:20 UT. On the TEC and ROTI maps, the black solid curves, red dashed curves and black contours denote the satellite paths of F18, the sunrise terminator and the magnetic dip latitudes, respectively. The black arrows on the TEC maps indicate the flying direction of DMSP satellite F18.

For the westward migration of the EPB and blob-like structures seen in TEC and ROTI maps, they were consistent with the topside plasma zonal drift around the plasma blob/EPB occurring region, which were predominantly westward (panels a4, b4 and c4 of Figure 3). For the movement of background plasma, it usually reverses from eastward to westward around midnight under geomagnetic quiet conditions (e.g., Huang et al., 2010). During magnetic storms, the storm-time electric field and/or disturbed thermospheric wind may also lead to westward zonal drift of the background plasma (e.g., Abdu, 2012; Li et al., 2021).

Regarding plasma blobs at the poleward sides of EPBs, previous studies suggested that they could be formed via plasma field-aligned diffusion during EPB generation process (e.g., Huang et al., 2014; Park et al., 2022; Wang et al., 2019). As suggested by Huang et al. (2014), the EPB initial generation would first drive the plasma density enhancement above the EPB structure over the magnetic equator, as schematically illustrated in Figure 4a. As the

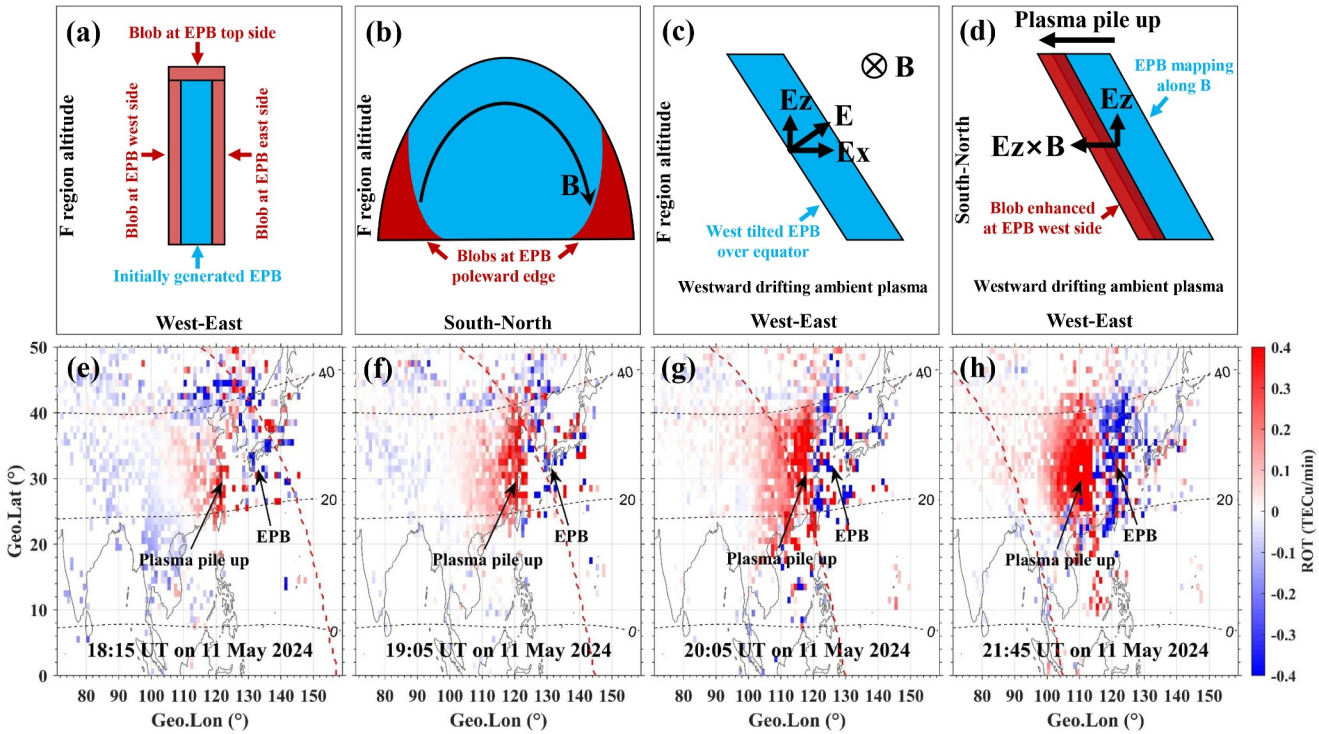

Figure 4. (a–d) Illustration of the super blob-like structure formation associated with EPB. (e–h) A sequence of ROT maps indicating the increase (positive ROT) and decrease (negative ROT) of TEC at different locations. The red dashed curve in each panel denotes the sunrise terminator. The black dashed contour denotes the magnetic dip latitudes.

EPB develops to higher altitude, the plasma density enhancement region would continue moving upward, and gradually expand poleward along the magnetic field lines. When the EPB is fully developed, the plasma blob will form at the poleward edges of the EPB structure, as schematically shown in Figure 4b. Under normal conditions, EPBs would mainly extend to low latitudes, thus most of the associated blobs were observed at low latitudes (e.g., Park et al., 2022). However, for the present case, the EPB extended to very high middle magnetic latitudes near ±40°, the corresponding blob-like structure could be reasonably formed at the magnetic latitude up to ±40° through a similar process.

For the blob-like structure at the EPB west side, there could be two possibilities. One is that the blob-like structure formed along with the initial generation of EPB structure "A" and then migrated westward together with the EPB and the background plasma. Previous simulation results showed that the plasma density may be enhanced by the sides of EPB structures when EPBs are initially generated (e.g., Huba & Liu, 2020; Yokoyama et al., 2015), as schematically illustrated in Figure 4a. Another possibility is that the blob-like structure was generated or enhanced during the westward drift process of the EPBs under certain EPB morphology, as schematically illustrated in Figures 4c and 4d. Generally, when an EPB forms over the magnetic equator, a polarization electric field develops with the direction perpendicular to the envelope of bubble, that is, from the west to the east wall of the bubble depletion structure (e.g., Huang et al., 2010; Ossakow & Chaturvedi, 1978). When the EPB structure is tilted, the polarization electric field inside the EPB depletion structures could lead to significant difference of particle zonal drift velocity inside the EPB structure from the ambient plasma (Huang et al., 2010). For the present case, the EPB structure sometimes showed a reversed C shape (e.g., at 17:45 UT in Figure 1), indicating a west-tilted morphology. For a west-tilted EPB structure (Figure 4c), the polarization electric field should have one component **Ez** pointing upward (Huang et al., 2010). The upward component **Ez** could map to higher latitudes along the magnetic field line and superimpose an additional westward velocity to the particle drift inside the EPB structure via $\mathbf{E} \times \mathbf{B}$. Owing to this superimposed westward drift, the particles inside the EPB depletion region would drift faster than the ambient plasma toward west and thus pile up on the west wall of the EPB structure, and finally contribute to the formation of the blob-like structure at the EPB west side (Figure 4d).

In order to visualize the plasma pile up process, the bottom panels of Figure 4 present a sequence of ROT maps, where positive (negative) ROT indicate the TEC increase (decrease) with time. On the ROT maps, EPB structures are mainly manifested as the region with fluctuated ROT values due to the existence of irregularities. At the west side of the EPB structure, the ROT was predominantly positive, indicating the plasma pile up process. Further, while comparing the plasma zonal drift measured by DMSP satellite F18 (Figure 3), it could be noted that the westward zonal drift was generally larger when the satellite fully passed the EPB structure (i.e., panel a4) than other time intervals when the satellite only partly passed (i.e., panel b4) or did not pass (i.e., panel c4) EPB structures. Whereas the zonal drifts were measured at different locations and time, their difference inside and outside EPB structures may partly indicate the influence of the polarization electric field inside the EPB structures on the particle zonal drift and the potential contribution to the plasma blob-like structures.

It is relevant to mention that whereas the morphology of the blob-like structures could be closely related to the EPB development, the essential particle sources required for their formation were also important. During magnetic storms, the background plasma density at middle latitudes could be enhanced by storm-time eastward electric field via the fountain effect originated over the magnetic equator, and/or equatorward neutral wind via field-aligned transportation from higher latitudes (e.g., Zhao et al., 2019). For the present case, the occurrence of super EPBs may indicate the possible presence of storm-time eastward electric field and/or equatorward neutral wind, which were suggested to enhance the Rayleigh-Taylor instability and favor EPB generation during magnetic storms (e.g., Huba & Liu, 2020; Otsuka et al., 2021; Sun et al., 2023). Whereas the true initiation of the TEC enhancement over the more eastern longitudes could not be well traced due to data gaps, a reasonable conjecture is that the background TEC over middle to low latitudes was enhanced due to the possible presence of storm-time eastward electric field and/or equatorward neutral wind, for example, over the longitudes more eastern than 150°E. Then due to the generation and development of the super EPB, the morphology of TEC enhancement region was modulated and finally formed the blob-like structures. From the bottom panels of Figure 4, the TEC increasing rate inside the blob-like structure became larger after sunrise, indicating that the photochemical production near sunrise also played a role to the additional enhancement of the blob-like structures.

5. Summary

We report a case of super ionospheric plasma blob-like structures occurring up to middle latitude around sunrise over East Asia during the May 2024 great geomagnetic storm, which was observed along with super ionospheric plasma bubbles with possible initiation at the more eastern longitudes after sunset. The blob-like structures created a region with TEC enhanced by up to 50 TECu, and migrated westward a few thousand kilometers together with the bubble. Different from most plasma blobs preferring to occur over low latitudes at the poleward edge of plasma bubbles, the blob-like structures in the present case occurred up to 40° magnetic latitudes and appeared at both the poleward and west sides of the plasma bubble. The blob-like structure at the poleward side of the bubble may be formed partly via plasma field-aligned diffusion associated with the bubble development. For the blob-like structure at the west side of the bubble, one possible mechanism is that it was formed along with the bubble initial generation, and/or enhanced accompanying the bubble evolution and westward drift under the polarization electric field inside the titled bubble structure. The results suggest that large-scale plasma depletion and blob structures could coexist from low to middle latitudes during the occurrences of super bubbles, and have implications for better understanding the sudden changes of plasma density in time and altitude observed by radar.

Data Availability Statement

The GNSS data were obtained from the Geophysics Center, National Earth System Science Data Center at BNOSE, IGGCAS (http://wdc.geophys.ac.cn/dbList.asp), the Chinese Meridian Project (http://data.meridianproject.ac.cn), the Geoscience Australia GNSS data repository (https://data.gnss.ga.gov.au/docs/), the UCSD GNSS database (ftp://garner.ucsd.edu/pub/rinex) and the online global TEC database (https://stdb2.isee.nagoya-u.ac.jp/GPS/GPS-TEC/). The Swarm data is available from the European Space Agency (https://swarm-diss.eo.esa.int/). The DMSP data were obtained from Madrigal database (http://cedar.openmadrigal.org/single). All the data used in this study are archived at the Beijing National Observatory of Space Environment, Institute of Geology and Geophysics, Chinese Academy of Sciences, and can be accessed at the WDC for Geophysics, Beijing (Sun, 2024).

Acknowledgments
This work was supported by the National Natural Science Foundation of China (42020104002), the Project of Stable Support for Youth Team in Basic Research Field, CAS (YSBR-018), the Solar-Terrestrial Environment Research Network (STERN) of Chinese Academy of Sciences, the International Partnership Program of Chinese Academy of Sciences (Grant 183311KYSB20200003), the Chinese Meridian Project, the JSPS KAKENHI (Grant 22K21345, 21H04518, and 20H00197), JSPS Bilateral Joint Research Projects No. JPJSBP120247202, and JSPS476 Core-to-Core Program, B. Asia-Africa Science Platforms. Work at MIT is supported by US NSF awards AGS-2033787, AGS-2149698, and AGS-1952737, and US NRL Grants N00014-23-1-2160 and N00014-24-1-2122, and NASA Grants 80NSSC21K1310, 80GSFC22CA011, and 80NSSC22K1013. The authors acknowledge the Integrated Research Center for Islands and Reefs Sciences, Chinese Academy of Sciences (http://www.djzx.ac.cn/) for the maintenance of several low latitude GNSS receivers.

References

Aa, E., Dzwill, P., Zhang, S.-R., & Erickson, P. J. (2024). A statistical analysis of the morphology of storm-enhanced density plumes over the North American sector. *Journal of Geophysical Research: Space Physics*, *129*(6), e2024JA032750. https://doi.org/10.1029/2024JA032750

Aa, E., Huang, W., Liu, S., Shi, L., Gong, J., Chen, Y., & Shen, H. (2015). A regional ionospheric TEC mapping technique over China and adjacent areas: GNSS data processing and DINEOF analysis. *Science China Information Sciences*, *58*(10), 1–11. https://doi.org/10.1007/s11432-015-5399-2

Abdu, M. A. (2012). Equatorial spread F/plasma bubble irregularities under storm time disturbance electric fields. *Journal of Atmospheric and Solar-Terrestrial Physics*, *75*(76), 44–56. https://doi.org/10.1016/j.jastp.2011.04.024

Beutler, G., Rothacher, M., Schaer, S., Springer, T. A., Kouba, J., & Neilan, R. E. (1999). The International GPS Service (IGS): An interdisciplinary service in support of Earth sciences. *Advances in Space Research*, *23*(4), 631–653. https://doi.org/10.1016/S0273-1177(99)00160-X

Choi, H.-S., Kil, H., Kwak, Y.-S., Park, Y.-D., & Cho, K.-S. (2012). Comparison of the bubble and blob distributions during the solar minimum. *Journal of Geophysical Research*, *117*(A4), A04314. https://doi.org/10.1029/2011JA017292

Foster, J. C. (1993). Storm time plasma transport at middle and high latitudes. *Journal of Geophysical Research*, *98*(A2), 1675–1690. https://doi.org/10.1029/92JA02032

Friis-Christensen, E., Lühr, H., Knudsen, D., & Haagmans, R. (2008). Swarm-an Earth observation mission investigating geospace. *Advances in Space Research*, *41*(1), 210–216. https://doi.org/10.1016/j.asr.2006.10.008

Haaser, R. A., Earle, G. D., Heelis, R. A., Klenzing, J., Stoneback, R., Coley, W. R., & Burrell, A. G. (2012). Characteristics of low-latitude ionospheric depletions and enhancements during solar minimum. *Journal of Geophysical Research*, *117*(A10), A10305. https://doi.org/10.1029/2012JA017814

Heelis, R. A., & Coley, W. R. (2007). Variations in the low- and middle-latitude topside ion concentration observed by DMSP during superstorm events. *Journal of Geophysical Research*, *112*(A8), A08310. https://doi.org/10.1029/2007JA012326

Huang, C.-S., de La Beaujardiere, O., Pfaff, R. F., Retterer, J. M., Roddy, P. A., Hunton, D. E., et al. (2010). Zonal drift of plasma particles inside equatorial plasma bubbles and its relation to the zonal drift of the bubble structure. *Journal of Geophysical Research*, *115*(A7), A07316. https://doi.org/10.1029/2010JA015324

Huang, C.-S., Foster, J. C., & Sahai, Y. (2007). Significant depletions of the ionospheric plasma density at middle latitudes: A possible signature of equatorial spread F bubbles near the plasmapause. *Journal of Geophysical Research*, *112*(A5), A05315. https://doi.org/10.1029/2007JA012307

Huang, C.-S., Le, G., de La Beaujardière, O., Roddy, P. A., Hunton, D. E., Pfaff, R. F., & Hairston, M. R. (2014). Relationship between plasma bubbles and density enhancements: Observations and interpretation. *Journal of Geophysical Research: Space Physics*, *119*(2), 1325–1326. https://doi.org/10.1002/2013JA019579

Huba, J. D., & Liu, H.-L. (2020). Global modeling of equatorial spread F with Sami3/WACCM-X. *Geophysical Research Letters*, *47*(14), e2020GL088258. https://doi.org/10.1029/2020GL088258

Kil, H., Choi, H.-S., Heelis, R. A., Paxton, L. J., Coley, W. R., & Miller, E. S. (2011). Onset conditions of bubbles and blobs: A case study on 2 march 2009. *Geophysical Research Letters*, *38*(6), L06101. https://doi.org/10.1029/2011GL046885

Kil, H., Paxton, L. J., Jee, G., & Nikoukar, R. (2019). Plasma blobs associated with medium-scale traveling ionospheric disturbances. *Geophysical Research Letters*, *46*(7), 3575–3581. https://doi.org/10.1029/2019GL082026

Kim, V. P., & Hegai, V. V. (2016). Low latitude plasma blobs: A review. *Journal of Astronomy and Space Sciences*, *33*(1), 13–19. https://doi.org/10.5140/JASS.2016.33.1.13

Klenzing, J. H., Rowland, D. E., Pfaff, R. F., Le, G., Freudenreich, H., Haaser, R. A., et al. (2011). Observations of low-latitude plasma density enhancements and their associated plasma drifts. *Journal of Geophysical Research*, *116*(A9), A09324. https://doi.org/10.1029/2011JA016711

Le, G., Huang, C.-S., Pfaff, R. F., Su, S.-Y., Yeh, H.-C., Heelis, R. A., et!al. (2003). Plasma density enhancements associated with equatorial spread F: ROCSAT-1 and DMSP observations. *Journal of Geophysical Research*, *108*(A8), 1318. https://doi.org/10.1029/2002JA009592

Li, G., Ning, B., Otsuka, Y., Abdu, M., Abadi, P., Liu, Z., et al. (2021). Challenges to equatorial plasma bubble and ionospheric scintillation short-term forecasting and future aspects in East and Southeast Asia. *Surveys in Geophysics*, *42*(1), 201–238. https://doi.org/10.1007/s10712-020-09613-5

Li, G., Ning, B., Zhao, B., Liu, L., Wan, W., Ding, F., et al. (2009). Characterizing the 10 November 2004 storm-time middle-latitude plasma bubble event in Southeast Asia using multi-instrument observations. *Journal of Geophysical Research*, *114*(A7), A07304. https://doi.org/10.1029/2009JA014057

Li, G., Ning, B., Zhao, X., Sun, W., Hu, L., Xie, H., et al. (2019). Low latitude ionospheric TEC oscillations associated with periodic changes in IMF Bz polarity. *Geophysical Research Letters*, *46*(16), 9379–9387. https://doi.org/10.1029/2019GL084428

Ma, G., & Maruyama, T. (2006). A super bubble detected by dense GPS network at east Asian longitudes. *Geophysical Research Letters*, *33*(21), L21103. https://doi.org/10.1029/2006GL027512

Maruyama, T., Ma, G., & Tsugawa, T. (2013). Storm-induced plasma stream in the low-latitude to midlatitude ionosphere. *Journal of Geophysical Research: Space Physics*, *118*(9), 5931–5941. https://doi.org/10.1002/jgra.50541

Ossakow, S. L., & Chaturvedi, P. K. (1978). Morphological studies of rising equatorial spread F bubbles. *Journal of Geophysical Research*, *83*(A5), 2085–2090. https://doi.org/10.1029/JA083iA05p02085

Otsuka, Y., Shinbori, A., Sori, T., Tsugawa, T., Nishioka, M., & Huba, J. D. (2021). Plasma depletions lasting into daytime during the recovery phase of a geomagnetic storm in May 2017: Analysis and simulation of GPS total electron content observations. *Earth and Planetary Physics*, *5*(5), 427–434. https://doi.org/10.26464/epp2021046

Oya, H., Takahashi, T., & Watanabe, S. (1986). Observation of low-latitude ionosphere by the impedance probe onboard the Hinotori satellite. *Journal of Geomagnetism and Geoelectricity*, *38*(2), 111–123. https://doi.org/10.5636/jgg.38.111

Park, J., Huang, C.-S., Eastes, R. W., & Coster, A. J. (2022). Temporal evolution of low-latitude plasma blobs identified from multiple measurements: ICON, GOLD, and madrigal TEC. *Journal of Geophysical Research: Space Physics*, *127*(3), e2021JA029992. https://doi.org/10.1029/2021JA029992

Park, J., Min, K. W., Lee, J.-J., Kil, H., Kim, V. P., Kim, H.-J., et al. (2003). Plasma blob events observed by KOMPSAT-1 and DMSP F15 in the low-latitude nighttime upper ionosphere. *Geophysical Research Letters*, *30*(21), 2114. https://doi.org/10.1029/2003GL018249

Park, J., Stolle, C., Lu¨hr, H., Rother, M., Su, S.-Y., Min, K. W., & Lee, J.-J. (2008). Magnetic signatures and conjugate features of low-latitude plasma blobs as observed by the CHAMP satellite. *Journal of Geophysical Research*, *113*(A9), A09313. https://doi.org/10.1029/2008JA013211

Pi, X., Mannucci, A. J., Lindqwister, U. J., & Ho, C. M. (1997). Monitoring of global ionospheric irregularities using the Worldwide GPS Network. *Geophysical Research Letters*, *24*(18), 2283–2286. https://doi.org/10.1029/97gl02273

Pimenta, A. A., Sahai, Y., Bittencourt, J. A., Abdu, M. A., Takahashi, H., & Taylor, M. J. (2004). Plasma blobs observed by ground-based optical and radio techniques in the Brazilian tropical sector. *Geophysical Research Letters*, *31*(12), L12810. https://doi.org/10.1029/2004GL020233

Spogli, L., Alberti, T., Bagiacchi, P., Cafarella, L., Cesaroni, C., Cianchini, G., et al. (2024). The effects of the May 2024 Mother's Day superstorm over the Mediterranean sector: From data to public communication. *Annals of Geophysics*, *67*, PA218. https://doi.org/10.4401/ag-9117

Sun, W. (2024). Ionospheric data during the May 2024 super geomagnetic storm. *WDC for Geophysics*. [Dataset]. https://doi.org/10.12197/2024GA014

Sun, W., Li, G., Lei, J., Zhao, B., Hu, L., Zhao, X., et al. (2023). Ionospheric super bubbles near sunset and sunrise during the 26–28 February 2023 geomagnetic storm. *Journal of Geophysical Research: Space Physics*, *128*(11), e2023JA031864. https://doi.org/10.1029/2023JA031864

Sun, W., Li, G., Zhang, S.-R., Hu, L., Dai, G., Zhao, B., et al. (2024). Regional ionospheric super bubble induced by significant upward plasma drift during the 1 December 2023 geomagnetic storm. *Journal of Geophysical Research: Space Physics*, *129*(6), e2024JA032430. https://doi.org/10.1029/2024JA032430

Sun, W., Wu, B., Wu, Z., Hu, L., Zhao, X., Zheng, J., et al. (2020). Ionise: An ionospheric observational network for irregularity and scintillation in East and Southeast Asia. *Journal of Geophysical Research: Space Physics*, *125*(8), e2020JA028055. https://doi.org/10.1029/2020JA028055

Wang, C. (2010). New chains of Space weather monitoring stations in China. *Space Weather*, *8*, S08001. https://doi.org/10.1029/2010SW000603

Wang, Z., Liu, H., Shi, J., Wang, G., & Wang, X. (2019). Plasma blobs concurrently observed with bubbles in the Asian-Oceanian sector during solar maximum. *Journal of Geophysical Research: Space Physics*, *124*(8), 7062–7071. https://doi.org/10.1029/2018JA026373

Xiong, C., Lühr, H., Sun, L., Luo, W., Park, J., & Hong, Y. (2019). Long-lasting latitudinal four-peak structure in the nighttime ionosphere observed by the Swarm constellation. *Journal of Geophysical Research: Space Physics*, *124*(11), 9335–9347. https://doi.org/10.1029/2019JA027096

Yokoyama, T., Jin, H., & Shinagawa, H. (2015). West wall structuring of equatorial plasma bubbles simulated by three-dimensional HIRB model. *Journal of Geophysical Research: Space Physics*, *120*, 8810–8816. https://doi.org/10.1002/2015JA021799-T

Yokoyama, T., Su, S.-Y., & Fukao, S. (2007). Plasma blobs and irregularities concurrently observed by ROCSAT-1 and Equatorial Atmosphere Radar. *Journal of Geophysical Research*, *112*(A5), A05311. https://doi.org/10.1029/2006JA012044

Zhang, S.-R., Nishimura, Y., Vierinen, J., Lyons, L. R., Knipp, D. J., Gustavsson, B. J., et al. (2023). Simultaneous global ionospheric disturbances associated with penetration electric fields during intense and minor solar and geomagnetic disturbances. *Geophysical Research Letters*, *50*(19), e2023GL104250. https://doi.org/10.1029/2023GL104250

Zhao, B., Yang, C., Cai, Y., Jin, Y., Liang, Y., Ding, F., et al. (2019). East-west difference in the ionospheric response of the March 1989 great magnetic storm throughout East Asian region. *Journal of Geophysical Research: Space Physics*, *124*(11), 9364–9380. https://doi.org/10.1029/2019JA027108